The Role of the Mechanical Factor in Stress Corrosion Cracking

Y. Katz
Nuclear Research Center Negev - Israel

Abstract

Stress corrosion cracking in Ti - aqueous NaCl system were studied. Materials included alpha, beta, and alpha-beta Ti-alloys. Information regarding the slow crack growth region, in pre-cracked fatigue specimens was accumulated. In addition the micro-mechanics of the crack growth was investigated by acoustic emission techniques. The combined experimental results, together with observed thermal effects, stimulated discussion on the mechanical driving force involved in stress corrosion cracking.

Introduction

Two major influences are involved in stress corrosion cracking (SCC), electrochemical and mechanical. Separation of these two components is difficult, still important for the evaluation of proposed models. For example, the acoustic technique included in the experimental procedure is an attempt to differentiate between the electrochemical mechanism and the brittle crack stage mechanism of the crack growth. Some aspects related to measurement of sonic emissions from environmentally induced cracks have been described elsewhere[1][2].
The purpose of the current study is mainly to emphasize the mechanical component and its contribution, as reflected on the macro and micro scale.

Experimental and Results

The work was carried out on Ti-75A and Ti-8Al-1Mo-1V, Ti-5Al-2.5Sn, Ti-13V-11Cr-3Al alloys, all in annealed condition. In order to enhance SCC, fatigue pre-cracked notch specimens were used in 3.5% NaCl aqueous solution as the active environment.
Slow crack growth rate as a function of the applied stress intensity factor were determined as well as fracture morphology observed by means of electron fractography. Crack velocities were measured on tapered specimens instrumented with stress wave emission set-up. The emitted stress waves were monitored during the environment tests, and then related to the crack propagation rate (Fig. 1).

Temperature effects on the crack growth were measured in temperature range, (5°C - 70°C) where the mechanical contribution was not expected to be severely affected.

Summarizing the experimental results in a general way, the delayed failures involved short times due to relatively high crack velocities. In the slow crack growth region, the velocity was dependent on the applied stress intensity factor, and the temperature. Relatively low apparent activation energies for crack growth were determined, dependent on the applied stress intensity factor.

The fracture mode in the slow crack growth region was in general transgranular cleavage, with evidence of striations, and distinct crystallographic fracture process. Stress wave activity correlated with the crack propagation rate and indicated discontinuous behaviour of the crack growth.

Discussion and Conclusions

The experimental result can be interpreted according to macro-mechanics concepts. Rice and Drucker[3] in an investigation on changes in stressed bodies due to void and crack growth, treated the mechanical aspects of SCC. Two important points should be mentioned concerning the active environment problem. First, the total potential energy of a stressed elastic body is changed by creation of new traction free surfaces due to material removal, assuming same load and displacement condition. Furthermore, potential energy is released in a process which introduces an extension of discontinuities in the loaded segment. Obviously, the mechanical energy associated with crack extension like in the case where a dissolution process takes place, is not the only factor to be considered. This leads to the second point, a drastic change in γ-the modified surface energy can lead to fracture, as illustrated in Fig. 2A. This schematic figure is based on Rices formulation for the energy release rate per unit crack extension, while P is the irreversible energy dissipation rate during a unit crack propogation in order to balance γ_m only L^e will be needed in the active medium. The assumption made is that the plastic flow behaviour is not affected strongly by the environment. Surplus mechanical energy is obtained which is increasing as the applied load is exceeding the values of L^e and approaching L^m.

Up to this point the reasons for the low stress intensity initiation of crack growth, and the role of the mechanical energy as a driving force for SCC have been considered. The approach for explaining the slow crack growth region is illustrated in Fig. 2B and follows the one originated by Irwin[4].

Assuming the discontinuous nature of SCC process as shown experimentally, the idea of an unstable running crack due to corrosion and mechanical effects on one side, and relaxation factors which will cause crack arrest on the other side, should be considered. In the figure G is the elastic energy release rate which has a linear trace and R the resistance energy term to crack propagation vs. crack length. In case of the environment, the crack will become unstable at σ^e_{crit} which is low, but a small increment of the crack will cause the extended tip to be characterized by the R curve. Time will be needed for the active medium to initiate the next step. The duration of the slow crack growth process cannot exceed more than C_{crit} where fracture will occur without the corrosive environment. Although the macro-concepts are descriptive, they are not concerned with the specific micro-mechanism taking place. Refinements are needed for the micro-mechanisms involved. It is important to mention that the fractographic observations, as well as the acoustic emission results in Ti systems are consistent with the concept of having a strong mechanical component involved in the fracture process. The rapid kinetics and the increase of amplitude and frequency of the stress waves with the applied stress intensity, support the idea that brittle fracture is progressing in the usual sense, but, enhanced at a lower stress.

The slow crack growth behaviour results from two origins, enhanced crack initiation and larger jump distances due to mechanical energy. Wood[5] followed similar experimental procedure, and found discontinuous cracking, and the influence of stress intensity factor on the stress waves amplitude and frequency, also in Al systems.

Referring to the low apparent activation energy a thermodynamic approach mentioned previously[1] for combined temperature and stress controlled rate process was applied. This expression for the crack propagation rate:

$$\frac{dc}{dt} = f(K) \exp - (Q-GAs)/RT$$

Problem Formulation and Results

The Ti-8-1-1 alloy seemed to be more susceptible to SCC. The initial condition were Ki/Kcrit = 0.32 (where Kcrit - stress intensity factor which cause the material to fail in the absence of an active chemical environment), with a velocity of about 1×10^{-3}in/sec at K/Kcrit about 0.4. The velocity was strongly dependent on K, furthermore a mechanically dominated portion started at about Ki/Kcrit = 0.8 which involved sharp increase of crack rate. The Ti-5-2.5 alloy had similar characteristics with the exception that up to Ki/Kcrit = 0.8 the crack velocity had a small dependence on K. In general Kcrit was not influenced by Ki and appeared more of a material constant considering the specimen thickness.

In order to analyse T_f (total time to failure) data, first the direct calculation of T_f was programmed for the SEN specimen.

Consider a notched specimen where K is given by:

$$K = F(c,W) = \sigma C^{\frac{1}{2}} \psi(c,W) \qquad (1)$$

where σ is the applied stress and $\psi(c,W)$ a correction for the specimen finite width. ψ can be expressed in different forms and was taken following the trigonometric function:(4)

$$\psi = 2 \left(\sin\frac{2\pi c}{2W} + \mathrm{Sec}\frac{2\pi c}{2W}\right) \qquad (2)$$

Assume that experimentally the crack propagation rate is determined and approximated by:

$$\frac{dc}{dt} = f(K) = m(\Delta K)^n \qquad (3)$$

$\Delta K = K - Ko$ and Ko is some reference level of K or in proper test conditions K_{iscc}.

Thus T_f can be obtained from the following expression:

$$T_f = \int_{c1}^{c2} \frac{dc}{f(K)} \qquad (4)$$

since practically it is more convenient to consider the crack length as a parameter due to the fact that c is directly measurable.

Let us first consider the case for Ko = 0, then for load controlled conditions:

$$T_f \alpha I/(2\sigma)^n$$

where I is the integral according to equation 4. Numerical integration was applied for I. Values regarding the nondimensional form of I are shown in theFigs 1,2 , and might serve the SEN specimen in general. For T_f, the numerical computation included the solution for C_i corresponding to Kcrit (equation 2). Fig 3 illustrates the T_f behaviour for different values of n.

Consider now the inverted problem, namely the determination of the rate dependency on K from a given T_f curve. In order to fullfill this purpose a function fit method was needed in addition to the direct computation program. Following some general ideas with regard to arbitrary function fit method(5)(6) a specific program was modified and utilized for the T_f curve evaluation.

Basically the fitting program follows the Newton-Raphson method of iteration, in a way, that a set of observed values can be checked and estimated by a proposed function. Specifically, the parameters $\bar{P}$ were

determined to satisfy the rate function in the least square sense, namely the minimization of $Q(\bar{P}_J)$ given by the equation:

$$Q(\bar{P}) = \sum_{i=1}^{N} (T_f^i \text{ cal} - T_f^i \text{ obs})^2 \, wi$$

where: T_f^i cal = calculated values according the direct analyses.

T_f^i obs = observed values for the total timeto failure.

wi = weight factors

Fig 4 shows the calculated and observed velocities for both materials, using n and m which give the nearest relative minimum for $Q(\bar{n},\bar{m})$.

Up to this point the Ko = 0 case was treated. No major changes were involved in the detailed programming for the more general case, where the range of K was considered. Solutions for n and m are shown in figs 5,6. Here the normalized form of T_f curve is illustrated which included in the fitting analysis just the single parameter n.

In both materials Ko was taken to be the threshold level as obtained experimetally from the T_f curves. For the Ti-8-1-1 alloy $Ko=24\times10^3 psi\sqrt{in}$. was taken while for Ti-5-2.5 alloy $Ko=40\times10^3 psi\sqrt{in}$. As expected the parameters m and n changed. Still here as well as for Ko=0 the parameters were in very close range to the experimental values figured by plotting the crack propagation rate data an a log-log scale. The crack rate tendency for both materials, namely, higher dependency on K for the Ti-8-1-1 alloy compared to the Ti-5-2.5 alloy as obtained experimentally, result clearly from the T_f curve analysis.

Discussion and conclusions

As mentioned the main point of the present study was to stress the evaluation pattern of the T_f curve. Evaluation of this type if possible provide important information considering relative susceptibility classification, as well as complimentary information to be effective, whenever proposed mechanisns are investigated and applied. Although the SEN specimen was studied, the work can easily be extended to other geometries and even to refinements of the crack rate function (equation 3), as long as K vs. crack length function is available.

As known extensive research activity concerning related problems have been reported in connection to fatigue crack propagation. However, the fact that SCC consists of delayed failure phenomena, or subcritical crack growth, does not reduce the need for SCC information, since the analogy to fatigue is basically limited.

In conclusion, the experimental results given in Figs 4,5,6 indicate that it is possible to distinguish between the twc materials by analyzing the T_f curves. Furthermore, the fundamental information regarding the crack growth dependency on K as established from the time to failure curve, was consistent with the direct velocity measurments. The use of fracture mechanics parameters was demonstrated, taking into account that the crack velocity curve and the T_f curves were obtained independently. Although two different geometries were utilized, the general behavior was well reflected by the total time to failure curve.

References

1. S. Mostovoy, P. B. Corsley and E. J. Ripling, J. of Materials 2 No. 3 p.661 (1967).
2. S. Mostovoy and E. J. Ripling, J. of Applied Polymer Sci 10 p. 1351 (1966).
3. J. E. Strawley and G. Gross, Materials Research and Standards 7 No. 4 p.155 (1967).
4. W. W. Gerberich and Y. Katz; Eng. Fructure Mechanics 1 p.569 (1969).
5. E. A. Crosbie and J. E. Monahan, ANE 208 Sept (1959).
6. B. S. Garbow ANL F102 July (1965).

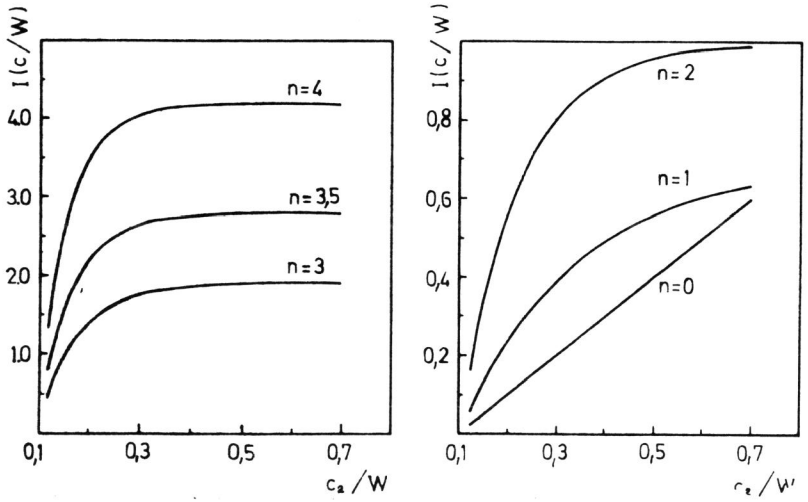

Fig. 1,2 Normalized integral values for the SEN specimen.

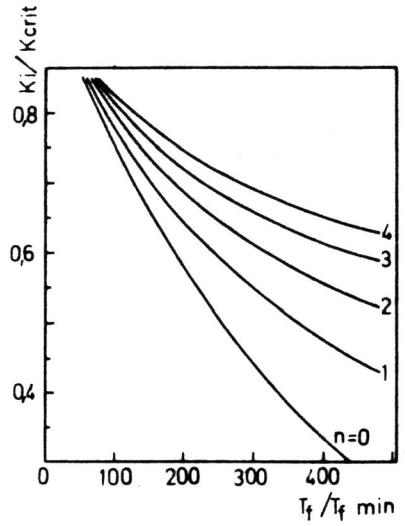

Fig. 3 Normalized T_f foe different n.
$K_o = 0$

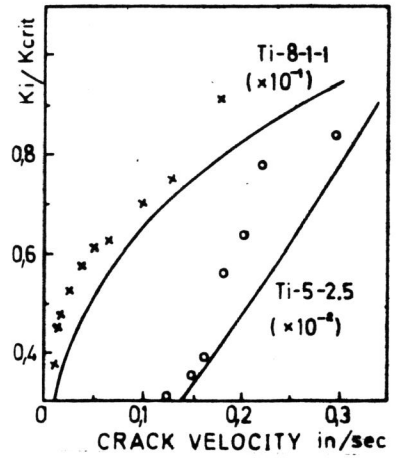

Fig. 4 Crack Velocity - observed and calculated.
Ti-8-1-1 n = 2.98
$m = 8.38 \times 10^{-17}$
Ti-5-2.5 n = 0.83
$m = 2.04 \times 10^{-7}$

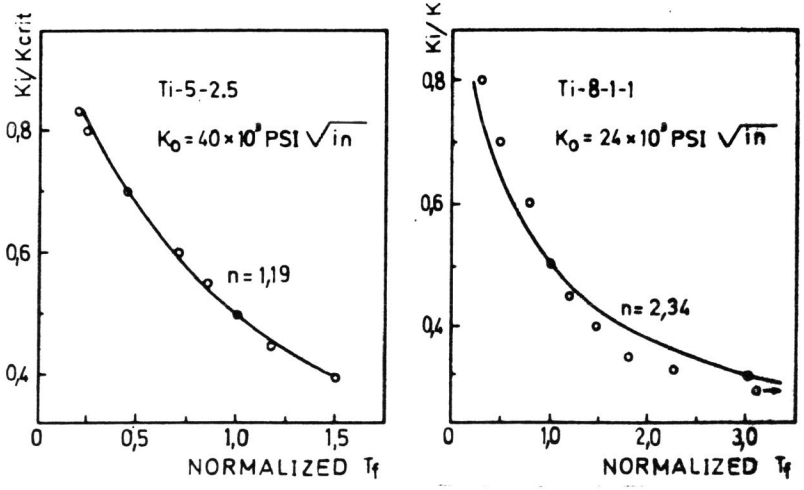

Fig. 5,6 Estimation of the Parameter n by best fit method.